Measurement of the Second-Order Hyperpolarizability of the Collagen Triple Helix and Determination of Its Physical Origin

Ariane Deniset-Besseau,[†] Julien Duboisset,[‡] Emmanuel Benichou,[‡] François Hache,[†] Pierre-François Brevet,[‡] and Marie-Claire Schanne-Klein*,[†]

Laboratoire d'Optique et Biosciences, Ecole Polytechnique, CNRS, INSERM U696, 91128 Palaiseau, France, and Laboratoire de Spectroscopie Ionique et Moléculaire, CNRS, Université Claude Bernard Lyon I, 69622 Villeurbanne, France

We performed Hyper−Rayleigh Scattering (HRS) experiments to measure the second-order nonlinear optical response of the collagen triple helix and determine the physical origin of second harmonic signals observed in collagenous tissues. HRS experiments yielded a second-order hyperpolarizability of 1.25×10^{-27} esu for rat-tail type I collagen, a surprisingly large value considering that collagen presents no strong harmonophore in its amino acid sequence. Polarization-resolved experiments showed intramolecular coherent contributions to the HRS signal along with incoherent contributions that are the only contributions for molecules with dimensions much smaller than the excitation wavelength. We therefore modeled the effective second-order hyperpolarizability of the 290 nm long collagen triple helix by summing coherently the nonlinear response of well-aligned moieties along the triple helix axis. This model was confirmed by HRS measurements after denaturation of the collagen triple helix and for a collagen-like short model peptide $[(Pro-Pro-Gly)_{10}]_3$. We concluded that the large collagen nonlinear response originates in the tight alignment of a large number of small and weakly efficient harmonophores, presumably the peptide bonds, resulting in a coherent amplification of the nonlinear signal.

Introduction

Collagen is the most abundant protein in mammals and represents around 25% of all proteins. Many genetically distinct collagen types have been described so far that are characterized by a specific organization and distribution in tissues.[1,2] Their common feature is the presence of triple helical domains: three left-handed polyproline II-like helices, called α-chains, are wrapped around one another in a ropelike right-handed superhelix.[3,4] Close packing is ensured by the presence of a glycine residue every third position in the α-chains, resulting in a $(Gly-X-Y)_n$ repeated structure. X and Y correspond mainly to proline and hydroxyproline residues that promote formation of polyproline II-like helices. The triple helix itself is stabilized by interchain hydrogen bonding, and its conformation was deduced from X-ray diffraction patterns using model triple-helical peptides such as $[(Pro-Pro-Gly)_{10}]_3$.[5−7]

Some of the collagens (types I, II, III, V, XI, XXIV, XXVII) self-assemble to form fibrils with diameters ranging from 10 to 300 nm. Those fibrils then organize in fibers and fascicles in a hierarchical way that is specific for each tissue. The major fibrillar collagen is collagen I whose helical domain is continuous over about 1000 amino acids. It is found in many tissues such as skin, tendon, bone, ligament, cornea, or arterial adventitia where it is often associated with other types of collagens. The other collagen types do not form fibrils since the triple-helical domains are interrupted by noncollagenous domains. Among them, type IV collagen forms a two-dimensional network found mainly in basement membranes.

As a fundamental brick of the architecture of tissues, collagen is crucial in the adaptive response to a variety of tissue injuries, such as infections, hypertension, mechanical stress, ischemia, cancer, immunological aggression, and burn. In such cases, the three-dimensional (3D) distribution of collagen within the extracellular matrix may be modified, thus altering the structure of affected organs and eventually leading to their functional failure. Characterizing collagen quantity and distribution during tissue remodeling is therefore of considerable interest. However, conventional techniques such as histological staining and immunochemical labeling are highly invasive, lack 3D resolution, and provide only semiquantitative phenomenological scores.

In that context, it is noteworthy that collagen fibers exhibit intrinsic second harmonic generation (SHG) signals in tissues, as first reported in 1986 in a rat-tail tendon.[8] SHG is a second-order nonlinear process where an intense pulsed laser source at frequency ω induces a nonlinear polarization in the sample which coherently radiates at harmonic frequency 2ω.[9−11] SHG was recently implemented in a multiphoton microscope setup, and SHG signals from collagen fibers were recorded in combination with two-photon excited fluorescence[12−25] and third-harmonic generation[26] to visualize the 3D morphology of thick unstained tissues. SHG microscopy indeed presents intrinsic 3D resolution like other nonlinear optical microscopies due to the spatial confinement of the conversion process at the focus of the laser beam. This so-called optical sectioning is more robust upon light scattering than confocal microscopy and enables improved depth penetration within tissues with the use of excitation wavelengths in the near-IR penetration window. Most importantly, the high specificity of SHG signals for fibrillar collagen results in a small background noise in SHG images and enables sensitive measurements of the fibrillar collagenous

* Corresponding author. Phone: +33 16933 5060. Fax: +33 16933 5084. E-mail: marie-claire.schanne-klein@polytechnique.edu.
    [†] Ecole Polytechnique.
    [‡] Université Claude Bernard Lyon I.

3D network.[25,27] The absence of any staining or labeling guarantees the reproducibility of these measurements so that SHG microscopy has been shown to be a sensitive tool to assess the progression of fibrotic pathologies.[24]

These measurements, however, were based on a phenomenological approach and determined only the extent of fibrillar collagen in the tissue by counting the number of voxels exhibiting a significant SHG signal. Indeed, SHG is a coherent optical process where signals scale with the squared molecular density and are highly sensitive to the organization of the molecules in the interaction volume. The heterogeneous 3D organization of collagen at the micrometer scale results in a complex relationship between the signal intensity and the number *and* the distribution of collagen molecules. Consequently, SHG microscopy does not provide any measurement of the quantity of collagen molecules yet. This difficulty has not been overcome by other approaches based on absolute measurements of the nonlinear susceptibility of collagenous tissues by comparison to nonlinear crystals[28−30] or calibration of the SHG signal as a function of the fibril's diameter by comparison to AFM images.[31] The main limitation in all these studies is the lack of quantitative data about the collagen second harmonic response at the molecular level.

Therefore, the first purpose of this study is to measure the second-order hyperpolarizability of the collagen triple helix using Hyper−Rayleigh Scattering (HRS) experiments. HRS is the standard technique for measurements of molecular second-order hyperpolarizabilities in the liquid phase.[32−34] Because of the overall isotropy of the medium, no coherent SHG signal can be recovered. However, owing to the orientational fluctuations of the molecules dispersed in the solution, a weak incoherent SH signal may still be detected. This signal intensity scales linearly with the molecular volume density because it is just the mere superposition of the SH intensities generated by the molecules. HRS therefore enables a straightforward measurement of the collagen second-order hyperpolarizability independently of the 3D organization of large and complex architectures. It requires nevertheless a sensitive setup since HRS intensities are much smaller than SHG ones and a careful normalization procedure to get absolute magnitudes.

The second purpose of this study is to gain insight into the physical origin of the second-order hyperpolarizability of collagen and to understand the role of its triple helical structure in the nonlinear optical response. For that purpose, we compare the nonlinear response of type I collagen from rat-tail in its native triple helical form and as single α-chains after denaturation. We also address the role of the length of the triple helical domain by studying a short collagenous-like model peptide and by modeling the nonlinear response as a function of the length of the triple helical domain.

This paper is organized as follows. The chemicals and the HRS experimental setup are presented briefly in the first section. The second section introduces the theoretical background, and the third one derives the expression of the effective hyperpolarizability measured in our HRS setup as a function of the length of the triple helical domain. The fourth section reports experimental results including polarization-resolved HRS data. Finally, in the Discussion section, we compare experimental results to theoretical predictions and propose a mechanism for the collagen hyperpolarizability.

Materials and Methods

Chemicals. Collagen I from rat-tail was supplied by Sigma Aldrich (product C7661) and solubilized in 0.5 mM acetic acid
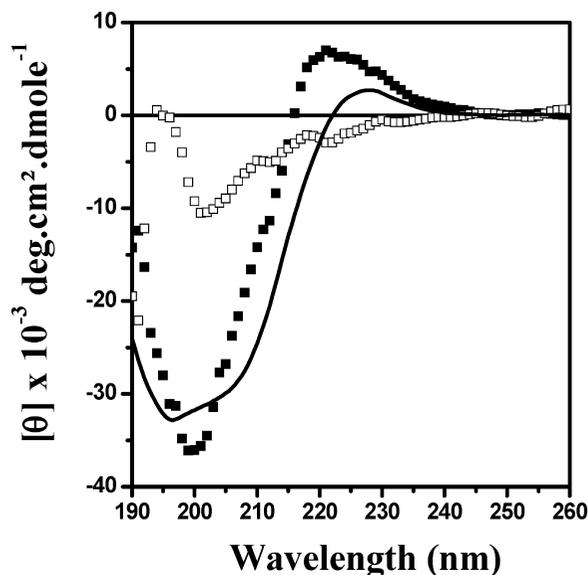

Figure 1. Circular dichroism spectra of 0.16 μM collagen solutions before (filled squares) and after (open squares) thermal treatment (50 °C for 10 min) and of the collagen-like polypeptide [(Pro-Pro-Gly)$_{10}$]$_3$ (solid line). All spectra are recorded at 10 °C using a 0.1 cm path-length quartz cell.

to obtain a 10 mg/mL stock solution. The acidic character of the solution (pH = 2.5) was aimed at preventing fibrillogenesis. Dilute solutions of 0.97−4.9 mg/mL (that is 3.4−17.4 μM) were prepared by weighting the solvent and the stock solution because of the high viscosity of collagen solutions. This concentration range was low enough to avoid any cooperative ordering of the triple helices to work with isotropic solutions and access molecular hyperpolarizabilities independently of the 3D organization.[35] For some experiments, thermal denaturation of the stock solution was performed at 50 °C during 10 min.

(Pro-Pro-Gly)$_{10}$ was supplied by Peptides International (product OPG-4006, (Pro-Pro-Gly)$_{10}$·9H$_2$O) with purity higher than 95%. It was solubilized in 0.05 mM acetic acid to obtain a 3.3 mg/mL stock solution of [(Pro-Pro-Gly)$_{10}$]$_3$ and self-organized to form triple helices. Then, it was diluted to 1.2−3.3 mg/mL (0.49−1.32 mM) solutions. All stock solutions were stored at 4 °C, 24 h before use.

CD Characterization. The conformation of these compounds was verified by recording circular dichroism (CD) spectra. Measurements were performed in a spectropolarimeter (CD6 Dichrograph, Horiba Jobin-Yvon) equipped with a variable-temperature unit, using 0.1 cm path-length quartz cells. Figure 1 shows spectra recorded at 10 °C. The CD spectrum from native collagen presents a negative peak at around 200 nm (π−π* amide transition) and a positive one at 220 nm (n−π* transition) that are characteristic for the triple helical structure.[36] The CD spectrum obtained after thermal treatment of the collagen solution presents only the negative peak. It confirms that the collagen is denatured and transformed into gelatin: the triple helical structure is deleted, and the solution is composed of detached α-chains that exhibit a polyproline II conformation. The CD spectrum of [(Pro-Pro-Gly)$_{10}$]$_3$ is similar to the one of native collagen, although the negative peak (201 nm) and the positive one (230 nm) are slightly red-shifted.[36,37] It confirms that the model peptide presents a triple helical structure.

Hyper−Rayleigh Scattering Setup. The Hyper−Rayleigh scattering setup is schematized in Figure 2. Excitation was provided by a femtosecond Ti:Sapphire laser (Mira 900, Coherent) delivering pulses with 180 fs duration at a repetition
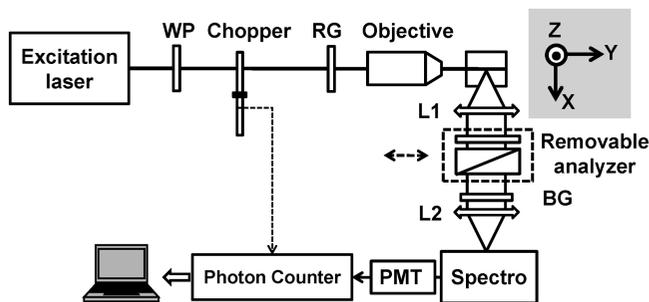
Second-Order Hyperpolarizability of Collagen

J. Phys. Chem. B, Vol. 113, No. 40, 2009 **13439**

Figure 2. Hyper−Rayleigh scattering experimental setup. WP: half-wave plate; RG and BG: color filters; L1 and L2: 25 mm focal length lenses; PMT: photon counting photomultiplier tube.

rate of 76 MHz. Wavelength was set to 790 nm with a mean power of 400 mW at the sample. We used a linear polarization whose polarization angle was adjusted by a half-wave plate to an angle γ from the vertical direction (Z axis in the laboratory frame, see Figure 3). This fundamental beam was focused with an 16x objective (NA = 0.32) into a quartz cell with 10 mm long optical path (Q107, Hellma). The laser spot diameter in the sample solution was approximately 40 μm. The HRS signal was collected at a right angle through a lens with 25 mm focal length and sent to a monochromator coupled to a cooled photomultiplier tube working in a gated photon counting regime (R943-02, Hamamatsu). Color filters were inserted to remove any unwanted harmonic light before the cell and fundamental light after the cell. For some experiments, the vertical or horizontal polarization state of the HRS signal was selected using a half-wave plate and a Glan polarizer. Owing to the low light level, the incoming beam was chopped at 130 Hz, so that the HRS intensity was corrected for the noise signal collected when the beam was blocked. HRS signals were integrated for typically 100 s at every experimental condition, and the laser power was monitored continuously to account for intensity fluctuations.

Theoretical Background

Symmetry Considerations. The second-order nonlinear molecular response is described by the second-order hyperpolarizability tensor $\beta(2\omega; \omega, \omega)$. The number of independent tensor components can be reduced when taking into account the molecular symmetry. The collagen triple helix is usually considered as a rigid molecule[38] with C_3 symmetry because of the three similar α-chains. In the present work, to simplify the molecular description, the symmetry was reduced to the $C_{\infty v}$ one. It satisfactorily reproduces polarization-resolved SHG experiments and reduces the number of independent tensor components.[14,39,40] Furthermore, considering the nonresonant character of the experimental conditions, the Kleinman symmetry is assumed to hold. Within these approximations, the only nonvanishing tensor elements are: β_{zzz} and $\beta_{zxx} = \beta_{zyy} = \beta_{xxz} = \beta_{yyz} = \beta_{xzx} = \beta_{yzy}$ in the molecular frame (x, y, z), where the z axis is the symmetry axis of the triple helix (see Figure 3).[9,10] In the following, we will also consider the collagen triple helix as a rodlike molecule with a single nonvanishing β_{zzz} component to further simplify the calculations.

The hyperpolarizability tensor is given in the molecular frame. To obtain the hyperpolarizability tensor in the laboratory frame (X, Y, Z), we use the following expression

$$\beta_{IJK} = \sum_{i,j,k} T_{Ii}T_{Jj}T_{Kk}\,\beta_{ijk} \qquad (1)$$

where T is the transfer matrix corresponding to Euler angles as displayed in Figure 3.

Internal Reference Method. The induced second-order dipole reads in the laboratory frame[9,10]

$$\mathbf{p}(2\omega) = \sum_{I,J,K} \beta_{IJK}E_J(\omega)E_K(\omega)\hat{\mathbf{I}} \qquad (2)$$

where $E_J(\omega)$ reads for the component along the Jth direction of the incident fundamental electric field and $\hat{\mathbf{I}}$ is the unitary vector along the Ith direction. The scattered harmonic field is then proportional to $\hat{\mathbf{X}} \times (\hat{\mathbf{X}} \times \mathbf{p}(2\omega))$ where $\hat{\mathbf{X}}$ is the collection direction of the HRS signal (see Figure 3). If the incident fundamental beam is vertically polarized and reads $\mathbf{E}(\omega) = E_0(\omega)\hat{\mathbf{Z}}$, one obtains

$$\mathbf{E}(2\omega) \propto (\beta_{YZZ}\hat{\mathbf{Y}} + \beta_{ZZZ}\hat{\mathbf{Z}})E_0(\omega)^2 \qquad (3)$$

The HRS signal is then obtained as the summation of the scattered harmonic intensities from all the molecules in the excitation volume[41,42]

$$I(2\omega) = GN_{\text{mol}}\langle|\beta_{YZZ}|^2 + |\beta_{ZZZ}|^2\rangle I(\omega)^2 \qquad (4)$$

where N_{mol} stands for the number of molecules in the excitation volume; G is a geometrical factor embedding all other constants; $I(\omega)$ is the fundamental intensity; and $< >$ stands for the averaging over the various molecular orientations determined by the Euler angles.

To determine quantitatively the second-order hyperpolarizability, we use the internal reference method where the HRS intensity of the collagen solution is normalized against the one of the bare solvent with known second-order hyperpolarizability. Setting $\beta = \langle|\beta_{YZZ}|^2 + |\beta_{ZZZ}|^2\rangle^{1/2}$ for collagen molecules and taking into account the contribution from the solvent molecules, the measured HRS signal reads

$$I(2\omega) = G(N_S\beta_S^2 + N_{\text{mol}}\beta^2)I(\omega)^2 \qquad (5)$$

where the index S stands for the solvent contribution. Since the HRS intensity scales linearly with the concentration of the solute, the second-order hyperpolarizability β is straightforwardly obtained from the linear fitting of the data obtained in a set of experiments where the HRS intensity is measured as a function of the solute concentration.

HRS Depolarization Ratio. We now consider that the incident beam polarization is at angle γ from the vertical axis in the laboratory frame (see Figure 3)

$$\mathbf{E}(\omega) = E_0(\omega)\cos\gamma\hat{\mathbf{Z}} + E_0(\omega)\sin\gamma\hat{\mathbf{X}} \qquad (6)$$

and that the HRS signal is analyzed in the vertical direction (superscript V) or in the horizontal one (superscript H). Using eq 2, one obtains the following expression for the HRS signal[43,44]

$$I^{V}(2\omega) = a^{V}(\cos\gamma)^4 + b^{V}(\cos\gamma)^2(\sin\gamma)^2 + c^{V}(\sin\gamma)^4 \qquad (7)$$
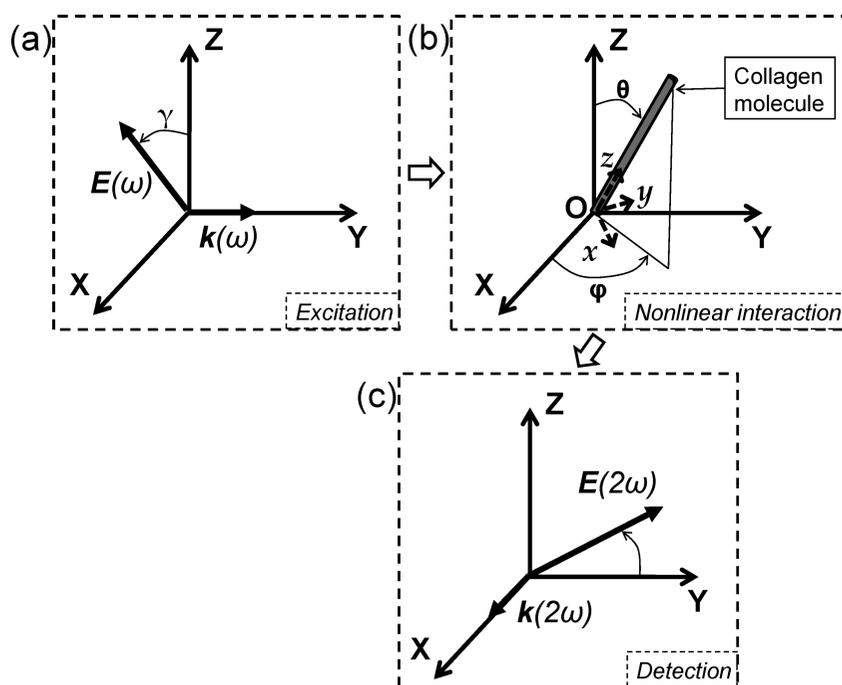
Figure 3. Laboratory and molecular frames. (a) Polarization angle γ of the excitation electric field $E(\omega)$. (b) Molecular frame and orientation of the collagen molecule in the laboratory frame (X, Y, Z) defined by Euler angles θ and φ. (c) Analysis of the polarization of the radiated electric field $E(2\omega)$.

with

$$a^{\mathrm{V}} = GN_{\mathrm{mol}}\langle|\beta_{ZZZ}|^2\rangle I(\omega)^2 \tag{8.a}$$

$$b^{\mathrm{V}} = GN_{\mathrm{mol}}\langle 4|\beta_{ZZX}|^2 + 2\mathrm{Re}(\beta_{ZZZ}\beta_{ZXX})\rangle I(\omega)^2 \tag{8.b}$$

$$c^{\mathrm{V}} = GN_{\mathrm{mol}}\langle|\beta_{ZXX}|^2\rangle I(\omega)^2 \tag{8.c}$$

Similar expressions are obtained for a horizontal analyzer. Polarization-resolved measurements then enable the determination of the depolarization ratio[45]

$$D = \frac{c^{\mathrm{V}}}{a^{\mathrm{V}}} = \frac{\langle|\beta_{ZXX}|^2\rangle}{\langle|\beta_{ZZZ}|^2\rangle} \tag{9}$$

This parameter depends on the various tensorial components of the molecular second-order hyperpolarizability in the molecular frame. We first consider the simplest case where the molecular second-order hyperpolarizability presents only one nonvanishing component β_{zzz}. Expression 1 gives: $\beta_{ZXX} = \cos\theta \sin^2\theta \cos^2\varphi\ \beta_{zzz}$ and $\beta_{ZZZ} = \cos^3\theta\ \beta_{zzz}$, and orientational averaging in expression 9 gives $D = 0.2$. Calculations for more complex symmetries have been reported in Brasselet et al.[45] We apply these calculations to the more realistic case of a $C_{\infty v}$ symmetry for the collagen triple helix as discussed above. Setting $u = \beta_{zxx}/\beta_{zzz}$, one obtains

$$D = \frac{3 - 4u + 20u^2}{15 + 36u + 72u^2} \tag{10}$$

Measurement of the depolarization ratio thus helps determine the symmetry of the molecule under study and the ratio of the various tensorial components.

Modeling of the Collagen Effective Hyperpolarizability

Intramolecular Coherent Contributions to the HRS Signal. The collagen triple helix is 1.5 nm in diameter and 290 nm long,[46] so that the optical length of the collagen molecule is close to the second harmonic wavelength. However, the hyperpolarizability formalism has been developed for molecules whose dimensions are much smaller than the wavelength. Consequently, we develop in the following an approach appropriate for longer molecules like collagen.

We consider a δl-long elementary moiety of the collagen molecule that is much smaller than the fundamental wavelength, so that the hyperpolarizability formalism strictly applies. The elementary moiety may be for instance a (Gly-X-Y) sequence of an α-chain. We assume that this moiety exhibits a $C_{\infty v}$ symmetry and that its second-order hyperpolarizability $\delta\beta$ is independent of the exact nature of the peptidic sequence. This assumption is consistent with the observation that similar SHG signals have been recorded from various types of fibrillar collagen: collagen type I, III, and V from tail-tendon, artery, skin, lung, etc. of kangaroo, rat, mouse, human, etc.[12−25] We then consider that the nonlinear response of the collagen triple helix results from the coherent summation of the nonlinear responses of all elementary moieties. This assertion is based on the two following hypotheses: (a) coherence is maintained within the collagen triple helix and (b) there are no collaborative effects between moieties.

In that framework, the HRS signal from a liquid solution of collagen is expected to present coherent intramolecular contributions besides the usual incoherent intermolecular contributions. Because of the macroscopic length of the collagen molecule, the account of those coherent intramolecular contributions requires a proper description of the retardation of the fields.

This has already been performed in gold nanoparticles and molecular aggregates where specific polarization-resolved HRS responses have been observed.[43,47] In particular, consideration of the field retardation in the frequency conversion mechanism has been shown to contribute to the b^V parameter only and not to the a^V and c^V ones (see eq 7) in some geometries. Following Nappa et al.,[43] we therefore consider the coherence ratio

$$\eta = \frac{a^V + c^V}{b^V} \quad (11)$$

This parameter has been shown to be equal to 1 when the HRS signal is purely incoherent, whereas one expects that $\eta \neq 1$ when the HRS response presents a coherent contribution.[47]

Effective Second-Order Hyperpolarizability of Collagen-Like Peptides. We now calculate the effective second-order hyperpolarizability β_{eff} resulting from the coherent summation of intramolecular elementary nonlinear responses. Because of the straight geometry of the collagen molecule, we can perform an exact calculation with a plane wave approximation. For that purpose, we use the geometry depicted in Figure 3 and consider vertically polarized excitation with no analyzer in the detection path. These calculations may be straightforwardly generalized to more complex configurations.

Similarly to expression 3, the nonlinear response from a moiety at position z along the collagen triple helix reads

$$\delta\mathbf{E}^{(z)}(2\omega) \propto (\delta\beta_{YZZ}\hat{\mathbf{Y}} + \delta\beta_{ZZZ}\hat{\mathbf{Z}})E^{(z)}(\omega)^2 \quad (12)$$

To take into account the propagation of the incident electric field along the collagen triple helix, we introduce the following phase factor

$$E^{(z)}(\omega) = E_0(\omega)\exp(i\mathbf{k}(\omega)\cdot\mathbf{z}) \quad (13)$$

with $\mathbf{k}(\omega) = 2\pi n_\omega/\lambda\hat{\mathbf{Y}}$ and $\hat{\mathbf{Y}}\cdot\mathbf{z} = z\sin\theta\sin\varphi$.

The harmonic field radiated by all the moieties then reads

$$\mathbf{E}(2\omega) = 3\int_0^L \delta\mathbf{E}^{(z)}(2\omega)\exp(-i\mathbf{k}(2\omega)\cdot\mathbf{z})dz \quad (14)$$

The factor 3 stands for the contributions of the three α-chains, and L stands for the molecular length. The phase factor due to the propagation of $\delta\mathbf{E}^{(z)}(2\omega)$ is calculated using the origin of the molecular frame as a reference (see Figure 3): $\mathbf{k}(2\omega) = (2\pi n_{2\omega})/(\lambda/2)\hat{\mathbf{X}}$ and $\hat{\mathbf{X}}\cdot\mathbf{z} = z\sin\theta\cos\varphi$.

Neglecting the index dispersion, one obtains

$$\mathbf{E}(2\omega) \propto 3(\delta\beta_{YZZ}\hat{\mathbf{Y}} + \delta\beta_{ZZZ}\hat{\mathbf{Z}})L\,\text{sinc}\left(\frac{k(2\omega)L}{2}(\sin\varphi - \cos\varphi)\sin\theta\right)E_0(\omega)^2 \quad (15)$$

The HRS signal is then obtained like in expression 4 as the summation of the scattered harmonic intensities from all the molecules in the excitation volume

$$\mathbf{I}(2\omega) = GN_{mol}\left\langle(|\delta\beta_{YZZ}|^2 + |\delta\beta_{ZZZ}|^2)(3L)^2 \times \text{sinc}^2\left(\frac{k(2\omega)L}{2}(\sin\varphi - \cos\varphi)\sin\theta\right)\right\rangle\mathbf{I}(\omega)^2 \quad (16)$$

We note that the HRS signal depends on the molecule length by the L factor and the sinc function. Further calculation of expression 16 requires the expression of $\delta\beta$ components in the molecular frame. We here consider the simplest case where only $\delta\beta_{zzz}$ is nonzero. Using expression 1, we obtain: $\delta\beta_{YZZ} = (\cos\theta)^2\sin\theta\sin\varphi\,\delta\beta_{zzz}$ and $\delta\beta_{ZZZ} = (\cos\theta)^3\,\delta\beta_{zzz}$. The HRS signal then reads

$$\mathbf{I}(2\omega) = GN_{mol}\beta_{eff}^2\mathbf{I}(\omega)^2 \quad (17)$$

with

$$\beta_{eff} = 3LK(L)\delta\beta_{zzz} \quad (18)$$

The function $K(L)$ stands for the orientational averaging

$$K^2(L) = \int_0^\pi d\theta\sin\theta\int_0^{2\pi}d\varphi[\cos^6\theta + \cos^2\theta\sin^2\theta\sin^2\varphi]\text{sinc}^2\left(\frac{k(2\omega)L}{2}(\sin\varphi - \cos\varphi)\sin\theta\right) \quad (19)$$

Similar expressions are derived for the $C_{\infty v}$ symmetry in the Supporting Information. β_{eff} then reads

$$\beta_{eff} = 3LK(L,u')\delta\beta_{zzz} \quad (20)$$

where u' stands for $u' = \delta\beta_{zxx} / \delta\beta_{zzz}$ similarly to eq 10, and $K(L,u')$ is given in the Supporting Information. Expressions 20 and A3 enable the comparison of the effective second-order hyperpolarizability β_{eff} from collagen-like peptides as a function of the length L of the triple helical domain. Figure 4 displays calculations of β_{eff} for $u' = 0$ (that is, when $\delta\beta_{zzz}$ is the only nonzero component) and $u' = 0.5$. They show that β_{eff} deviates from a linear behavior from $L \approx 50$ nm on as a consequence of the consideration of the field retardation. The results obtained for $L = 290$ nm provide the second-order hyperpolarizability expected for type I collagen from rat-tail. These results are normalized to the values obtained for a 8.6 nm long model peptide to eliminate all parameters except u'. This length was chosen because it corresponds to [(Gly-Pro-Pro)$_{10}$]$_3$ since the helical pitch of an α-chain is 0.86 nm long.[7,48] Note that we studied the model peptide [(Pro-Pro-Gly)$_{10}$]$_3$ that is the most usual reference peptide. This peptide is equivalent to [(Gly-Pro-Pro)$_{10}$]$_3$ for this study since we do not access the sign of the hyperpolarizability. One then obtains $\beta_{collagenI}/\beta_{PPG10} = 15.8$ for $u' = 0$ and $\beta_{collagenI}/\beta_{PPG10} = 12.7$ for $u' = 0.5$. A linear behavior would provide $\beta_{collagenI}/\beta_{PPG10} = 33.7$ since the triple helical domain of collagen I corresponds to [(Gly-X-Y)$_{337}$]$_3$.[46]

Experimental Results

Measurement of the Second-Order Hyperpolarizability. Figure 5a displays the HRS signal from solutions of rat-tail type I collagen in 0.5 M acetic acid as a function of the spectrometer wavelength. No background fluorescence is observed, so that the HRS intensity is straightforwardly obtained as the peak
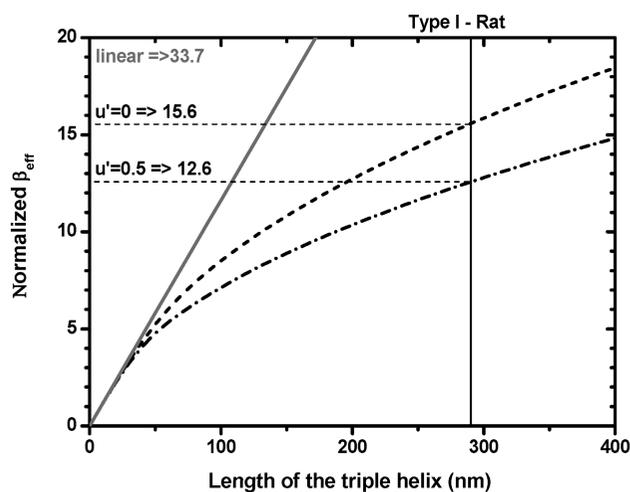
Figure 4. Theoretical calculations of $\beta_{eff}(L)$. β_{eff} is plotted as a function of the length L of the triple helical domain. Results are normalized to the β_{eff} obtained for [(Pro-Pro-Gly)$_{10}$]$_3$. Values are indicated for $L = 290$ nm that corresponds to type I collagen from rat-tail. Calculations are performed using a $C_{\infty v}$ symmetry with $u' = 0$ (dashed line) and $u' = 0.5$ (dot-dashed line). Linear behavior is indicated as for comparison (gray solid line).

intensity after subtraction of the dark background. The solvent signal is also displayed for comparison and used as an internal reference for quantitative measurements. For that purpose, we verified that acetic acid presents the same response as bare water and used the water second-order hyperpolarizability published in the literature,[49] namely, $\beta_{water} = 0.56 \times 10^{-30}$ esu. Figure 5b displays the collagen HRS intensity normalized to the solvent intensity as a function of the collagen concentration. As expected, it shows a linear behavior indicating the absence of artifacts due to molecular interactions. Linear fitting of the data provides the absolute value of the collagen second-order hyperpolarizability: $\beta_{collagen} = (1.25 \pm 0.05) \times 10^{-27}$ esu. Measurements were repeated three times over the full range of concentrations using new solutions for each set of experiments, and we obtained consistent results within the error bar. Excitation was vertically polarized, and we used no analyzer for these measurements, such that $\beta = \langle |\beta_{YZZ}|^2 + |\beta_{ZZZ}|^2 \rangle^{1/2}$, with the tensorial components given in the laboratory frame.

We performed the same measurements for denatured collagen. The triple helical structure has been destroyed by the thermal treatment, and the solution is composed of detached left-handed helical α-chains. Figure 5c displays the HRS intensity as a function of the concentration of α-chains that is 3-fold the initial concentration of triple helices. Experimental data show a linear behavior as for native collagen. Linear fitting then yields: $\beta_{denat\ collagen} = (1.70 \pm 0.20) \times 10^{-28}$ esu which is 7.4 less than for native collagen.

HRS experimental data for [(Pro-Pro-Gly)$_{10}$]$_3$ are displayed in Figure 5d. Higher concentrations than for the former experiments were required to obtain HRS signals larger than the solvent signal. We determined $\beta_{PPG10} = (9.9 \pm 0.6) \times 10^{-29}$ esu which is 12.6 less than for native collagen.

Polarization-Resolved HRS Experiments. We performed polarization-resolved HRS experiments to measure the depolarization ratio: $D = c^V / a^V$ and the coherence ratio $\eta = (a^V + c^V) / b^V$. For that purpose, we tuned the polarization angle of the excitation beam and selected the vertically polarized HRS signal. Figure 6 displays vertically polarized HRS intensity from a 5.0 mg/mL solution of native collagen and from the solvent. The difference between these two signals amounts to the

polarized response of collagen. Fitting of these data using eq 7 yields the parameters a^V, b^V, and c^V and then the ratios D and η. Results for native collagen, denatured collagen, and [(Pro-Pro-Gly)$_{10}$]$_3$ are summarized in Table 1, along with the β_{eff} values. We verified that $D \approx 0.2$ and $\eta \approx 1$ for the solvent which confirms that there are no polarization artifacts. We measured $D \neq 0.2$ for all other molecules under study. It indicates that their second-order hyperpolarizability tensor cannot be reduced to one component and must be described by a more complex symmetry group. We measured $\eta \approx 1$ for [(Pro-Pro-Gly)$_{10}$]$_3$, as expected for this short molecule, but $\eta \neq 1$ for native and denatured collagens, which indicates the presence of coherent effects within these molecules.

Discussion

Our experiments aimed at measuring the second-order hyperpolarizability of native and denatured type I collagen and of the short collagen-like model peptide [(Pro-Pro-Gly)$_{10}$]$_3$. To determine the physics of the collagen nonlinear response, we now discuss the assumptions used in the theoretical section according to our experimental results.

Our first assumption concerned the symmetry framework used for modeling the nonlinear response. We used a $C_{\infty v}$ symmetry for the hyperpolarizability tensor and calculated the depolarization ratio as a function of $u = \beta_{zxx} / \beta_{zzz}$ using eq 10. Figure 7 compares these theoretical calculations to the depolarization ratios measured for native collagen and for [(Pro-Pro-Gly)$_{10}$]$_3$. Experimental data can be matched to the theoretical calculations to estimate u. When taking into account the experimental error bars, we obtain the following estimations: $0.1 < u_{collagen} < 0.2$ or $0.5 < u_{collagen} < 0.9$ and $0.2 < u_{PPG10} < 0.7$. These results confirm that the collagen triple helix can be described within the $C_{\infty v}$ symmetry framework and indicate that β_{zxx} is not negligible compared to β_{zzz}.

Similar polarization-resolved experiments have been reported for SHG microscopy in the literature.[14,30,39,50−52] Measurement of depolarization ratios in SHG microscopy yielded $0.4 \leq (\chi_{zxx}/\chi_{zzz}) \leq 0.8$ for fibrillar collagen. If considering that all collagen molecules are aligned in the same direction within the fibrils, the second-order susceptibility tensor χ should reflect the symmetry of the second-order hyperpolarizability tensor β. Therefore, we expect that the depolarization ratio measured at the molecular scale using the HRS experiments is equal to the depolarization ratio measured in SHG microscopy within fibrils. We observe that it is qualitatively the case.

Our second assumption was that the nonlinear response of collagen arises from elementary moieties within the α-chains. In that respect, we expect that the second-order hyperpolarizability of native collagen is 3-fold the one of denatured collagen because native collagen is composed of three α-chains tightly interwoven in a triple helix whereas denatured collagen is composed of detached α-chains. Experimentally, we measured a ratio of 7.4 which is larger than the theoretical expectation, yet in qualitative agreement.

This quantitative discrepancy may be attributed to a smaller response of denatured collagen because single α-chains are less rigid than triple helices and may partially arrange in a random coil. The harmonic electric fields radiated by all the elementary moieties in the α-chain may therefore interfere in a destructive way, resulting in smaller effective second-order hyperpolarizability. Alternatively, intramolecular coherence may be partially lost in denatured collagen: the effective second-order hyperpolarizability measured for denatured collagen would then result from incoherent summation of the responses from molecular
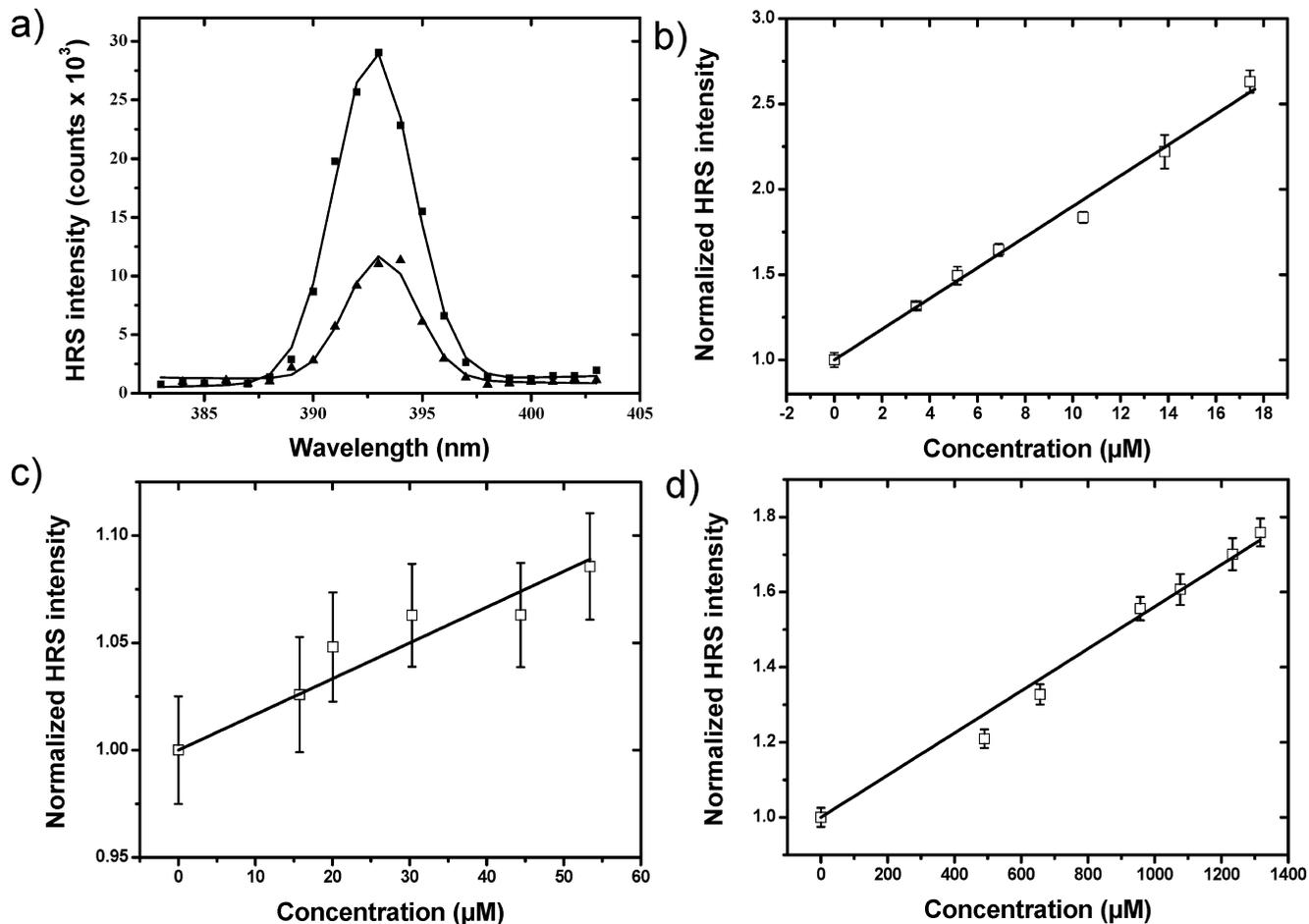
Second-Order Hyperpolarizability of Collagen

J. Phys. Chem. B, Vol. 113, No. 40, 2009 **13443**

Figure 5. HRS experimental results: (a) HRS intensity as a function of the harmonic wavelength for a 17.4 μM solution of native type I collagen from rat-tail (4.9 mg/mL, solid squares) and for the solvent (0.5 M acetic acid, solid triangles). (b) HRS intensity of native collagen normalized to the solvent intensity as a function of the concentration. The solid line is a linear fitting using eq 5. (c) Same as (b) for denatured collagen. (d) Same as (b) for the $[(\text{Pro-Pro-Gly})_{10}]_3$ model peptide.
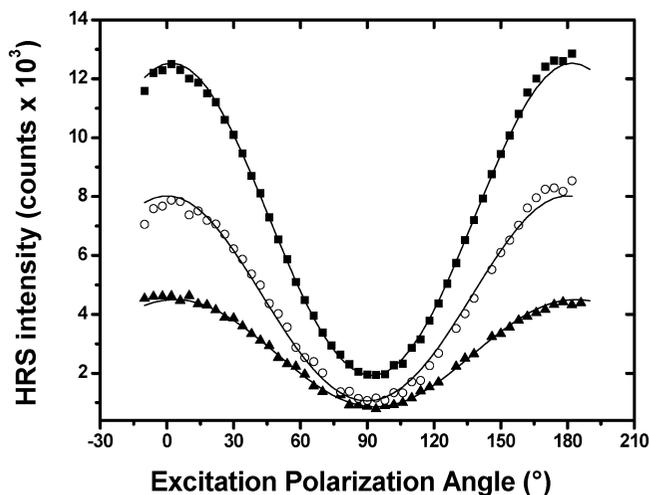

Figure 6. Vertically polarized HRS signal as a function of the polarization angle γ of the incoming beam as defined in Figure 3, for 17.4 μM native collagen solution (5 mg/mL, solid squares) and for solvent (0.5 acetic acid, solid triangles). Open circles represent the difference between both signals. Solid lines correspond to fitting with eq 7.

moieties and decrease compared to the coherent summation operating in the rigid triple helix. Nevertheless, intermolecular coherent effects are still a major contribution as shown by $\eta \neq 1$ (see Table 1) and by the qualitative agreement between the measured ratio and the theoretical prediction based on purely coherent contributions. Finally, we note that this partial coherence loss and/or partial random coil arrangement impede the discussion of the symmetry properties of denatured collagen. We still deduce from the depolarization ratio $D \neq 0.2$ that the hyperpolarizability tensor does not reduce to one nonzero component β_{zzz}.

Finally, comparing the effective second-order hyperpolarizabilities: 1250×10^{-30} esu measured for native type I collagen from rat-tail and 99×10^{-30} esu measured for $[(\text{Pro-Pro-Gly})_{10}]_3$, we obtain a ratio of 12.6. This ratio must be compared to the theoretical calculation for $L = 290$ nm (rat-tail type I collagen) normalized to the one for $L = 8.6$ nm ($[(\text{Pro-Pro-Gly})_{10}]_3$). These calculations depend on the symmetry of the hyperpolarizability tensor. Considering a $C_{\infty v}$ symmetry with $u' = 0$ and $u' = 0.5$ as displayed in Figure 4, the best agreement is obtained for $u' = 0.5$ and yields a theoretical ratio of 12.7 very close to the experimental one. Moreover, the value $u' = 0.5$ lies within the range deduced from the measurements of the depolarization ratio.

So, comparison of our experimental data to theoretical calculations consistently demonstrates that the collagen triple helix can be described in the $C_{\infty v}$ symmetry framework with a non-negligible $\delta\beta_{zxx} / \delta\beta_{zzz}$ ratio and that the collagen HRS intensity presents coherent intramolecular contributions. The agreement between experimental results and theoretical calculations using $u' = 0.5$ is excellent. However, theoretical calculations have to be considered carefully. First, the collagen

TABLE 1: Effective Second-Order Hyperpolarizability β_{eff}, Depolarization Ratio D, and Coherence Ratio η for the Solvent, Native, and Denatured Type I Collagen from Rat-Tail and [(Pro-Pro-Gly)$_{10}$]$_3$ Model Peptide

	solvent (0.5 M acetic acid)[a]	native collagen (type I, rat-tail)	denatured collagen (type I, rat-tail)	[(Pro-Pro-Gly)$_{10}$]$_3$
$\beta_{\text{eff}} = \langle\|\beta_{YZZ}\|^2 + \|\beta_{ZZZ}\|^2\rangle^{1/2}$ (10^{-30} esu)	0.56	1250 ± 50	170 ± 20	99 ± 6
$D = c^V / a^V$	0.18 ± 0.01	0.135 ± 0.015	0.29 ± 0.08	0.115 ± 0.015
$\eta = (a^V + c^V) / b^V$	0.97 ± 0.03	1.08 ± 0.06	0.89 ± 0.24	1.00 ± 0.03

[a] The β_{eff} indicated for the solvent is the value for water taken from ref 49 and used as an internal reference.
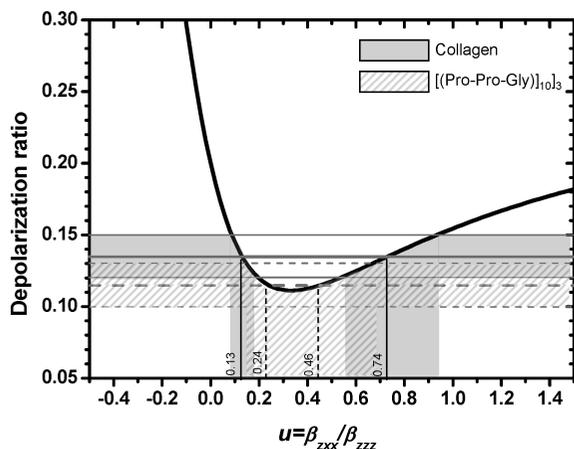
Figure 7. Comparison of experimental and theoretical depolarization ratios. The depolarization ratio given by eq 10 is plotted as a function of the ratio of the two nonvanishing tensor components within the $C_{\infty v}$ symmetry framework (black solid line). It is compared to the experimental data measured for native type I collagen from rat-tail (solid gray line) and the [(Pro-Pro-Gly)$_{10}$]$_3$ model peptide (gray dashed line). Thinner lines indicate the experimental error bars.

molecule does not strictly exhibit a $C_{\infty v}$ symmetry, and some tensorial components, for instance, the chiral components,[27] are neglected in that framework. The Kleinmann symmetry may also not be strictly verified[53] although polarization-resolved data from SHG microscopy have evidenced only slight deviations from the Kleinmann symmetry in collagen fibrils.[30] Second, although usually considered as a rigid molecule, collagen is a semiflexible polymer with a persistence length of about 160 nm.[35,54] Consequently, bending of the molecule apart from its main axis may result in uncertainties in the calculation. Third, the [(Pro-Pro-Gly)$_{10}$]$_3$ model peptide used as a reference may not be totally organized in triple helices which would result in a smaller effective hyperpolarizability. However, we expect that this effect is limited since the CD spectrum indicates that [(Pro-Pro-Gly)$_{10}$]$_3$ presents predominantly a triple helical structure. Fourth, the helical pitch of the α-chain may differ a little bit from the 0.86 nm value used for the calculations as it depends on various chemical parameters.[55] The refractive index may also differ from the water value 1.33 used for the calculations, or it may exhibit nonvanishing dispersion. However, we do not expect these parameters to significantly change our calculations. For instance, calculations using a refractive index $n = 1.37$ that corresponds to corneal collagenous tissue[56] result in a ratio of 12.6 for $u' = 0.5$. Similarly, a $\Delta n = -0.03$ dispersion[29] results in a <1% change in the calculated ratio. To summarize, our data cannot provide the exact value of $u' = \delta\beta_{zxx} / \delta\beta_{zzz}$, but they show that it is close to 0.5 and that the collagen second-order hyperpolarizability is definitively not limited to only one major nonvanishing component.

All above considerations demonstrate that the nonlinear response of the collagen triple helix originates in molecular moieties of the α-chains with dimensions much smaller than the optical wavelength. The second harmonic fields radiated by

all moieties sum predominantly in a constructive way because of the relative rigidity of the collagen triple helix that ensures alignment of these elementary harmonophores along the same direction. Furthermore, the collagen triple helix is a highly compact structure[7] so that coherent amplification is strikingly efficient and results in a large effective second-order hyperpolarizability as measured experimentally. Yet, the effective second-order hyperpolarizability shows a sublinear behavior as a function of the number of elementary harmonophores. Indeed, the length of the triple helical domain is of the same order of magnitude as the optical wavelength (see Figure 4), and retardation of the fields must be taken into account.

This mechanism of coherent amplification is consistent with the chemical structure of the collagen triple helix. Electronic delocalization along the α-chains or between the α-chains within the triple helix is unlikely. Accordingly, intramolecular cooperative effects are expected to be negligible, and nonlinearities are expected to be confined to one or a few amino acids. The exact location of the molecular moieties responsible for the nonlinearity is not clearly established. Noteworthy, glycine, proline, and hydroxyproline that are the major amino acids in the collagen sequence are not expected to present strong nonlinearities. Furthermore, large SHG signals were observed in tissues from various mammals and for many types of collagens, independently of the exact amino acid sequence. Therefore, the nonlinear response is probably not related to a particular amino acid but to the peptide bond itself. This hypothesis is in agreement with published data from sum frequency vibrational spectroscopy[40] and from polarization-resolved SHG microscopy.[51,52,57] To verify this assumption, we calculated the depolarization ratio assuming that the nonlinear response of the peptide bond is aligned along the α-chains (see Supporting Information).[51,52,57] We obtained a perfect agreement with the experimental data. That encouraging result shows that advanced theoretical calculations using quantum chemistry approaches would be of strong interest to certify the molecular origin of the nonlinearity.

Conclusion

In this paper, we successfully measured the second-order hyperpolarizability of type I collagen from rat-tail using HRS experiments: $\beta_{\text{collagen}} = (1.25 \pm 0.05) \times 10^{-27}$ esu. This value was unambiguously determined using the internal reference method over a wide range of concentrations.

Moreover, we demonstrated that the collagen nonlinear response originates in small molecular moieties that presumably correspond to the peptide bonds. The compactness and rigidity of the triple helix ensures that many of those harmonophores are well-aligned along the molecular axis, resulting in an efficient coherent amplification of the nonlinear signal. This effect is similar to the coherent summation of SH radiations from all collagen triple helices within fibrils, leading to large SHG signals for fibrillar collagens. In contrast, nonfibrillar collagens show vanishing signals since they are less dense and present a centrosymmetrical organization.[25,27] In summary, the

Second-Order Hyperpolarizability of Collagen

J. Phys. Chem. B, Vol. 113, No. 40, 2009 **13445**

mechanism leading to large SHG signals in collagen is the same at the molecular scale and at the supramolecular scale since the hierarchical structure of collagenous fibers is characterized by a high density and directionality at all the organization levels. This mechanism is not related to the presence of strong harmonophores but to the tight alignment of a large number of moderate harmonophores.

Our measurements of rat-tail type I collagen might be generalized to other collagens since the nonlinear response mainly depends on the length of the triple helical domain, not on the exact peptidic sequence. We expect similar effective second-order hyperpolarizability for all type I collagen molecules that are characterized by a 290 nm long triple helical domain. Moreover, our calculations provide a benchmark for the second-order hyperpolarizability of other collagen types once the length of the triple helical domain is known. Our measurements are therefore a major step toward quantitative second harmonic imaging of collagenous tissues.

More generally, the approach we developed for the collagen triple helix may be applied to any nonlinear optical object that can be modeled by a rigid rod with dimensions comparable to the optical wavelength. These objects could be other biological molecules or inorganic materials like nanowires.

Supporting Information Available: Derivation of the effective hyperpolarizability for $C_{\infty v}$ symmetry and derivation of the depolarization ratio of the collagen triple helix. This material is available free of charge via the Internet at http://pubs.acs.org.

References and Notes

(1) Hulmes, D. J. S. *J. Struct. Biol.* **2002**, *137*, 2–10.
(2) Kadler, K. E.; Baldock, C.; Bella, J.; P., R.; Boot-Handford, *J. Cell Sci.* **2007**, *120*, 1955–1958.
(3) Ramachandran, G. N.; Kartha, G. *Nature* **1955**, *176*, 593–5.
(4) Rich, A.; Crick, F. H. *J. Mol. Biol.* **1961**, *3*, 483–506.
(5) Okuyama, K.; Arnott, S.; Takayanagi, M.; Kakudo, M. *J. Mol. Biol.* **1981**, *152*, 427–43.
(6) Bella, J.; Eaton, M.; Brodsky, B.; Berman, H. M. *Science* **1994**, *266*, 75–81.
(7) Beck, K.; Brodsky, B. *J. Struct. Biol.* **1998**, *122*, 17–29.
(8) Freund, I.; Deutsch, M.; Sprecher, A *Biophys. J.* **1986**, *50*, 693–712.
(9) Boyd, R. W. *Nonlinear optics*; Academic press: London, 2003.
(10) Shen, Y. R. *The principles of nonlinear optics*; Wiley: New York, 1984.
(11) Eisenthal, K. B. *Chem. Rev.* **2006**, *106*, 1462–1477.
(12) Campagnola, P. J.; Millard, A. C.; Terasaki, M.; Hoppe, P. E.; Malone, C. J.; Mohler, W. A *Biophys. J.* **2002**, *82*, 493–508.
(13) Zoumi, A.; Yeh, A.; Tromberg, B. J. *Proc. Natl. Acad. Sci. U.S.A.* **2002**, *99*, 11014–11019.
(14) Stoller, P.; Reiser, K. M.; Celliers, P. M.; Rubenchik, A. M *Biophys. J.* **2002**, *82*, 3330–3342.
(15) Brown, E.; McKee, T.; diTomaso, E.; Pluen, A.; Seed, B.; Boucher, Y.; Jain, R. K. *Nat. Med.* **2003**, *9*, 796–800.
(16) Cox, G.; Kable, E.; Jones, A.; Fraser, I.; Marconi, K.; Gorrell, M. D. *J. Struct. Biol.* **2003**, *141*, 53–62.
(17) König, K.; Riemann, I. *J. Biomed. Opt.* **2003**, *8*, 432–439.
(18) Zipfel, W. R.; Williams, R. M.; Christie, M.; Nikitin, A. Y.; Hyman, B. T.; Webb, W. W. *Proc. Natl. Acad. Sci. U.S.A.* **2003**, *100*, 7075–7080.
(19) Zoumi, A.; Lu, X.; Kassab, G. S.; Tromberg, B. J. *Biophys. J.* **2004**, *87*, 2778–2786.
(20) Boulesteix, T.; Pena, A. M.; Pagès, N.; Godeau, G.; Sauviat, M.-P.; Beaurepaire, E.; Schanne-Klein, M. C. *Cytometry* **2006**, *69A*, 20–26.
(21) Kirkpatrick, N. D.; Andreou, S.; Hoying, J. B.; Utzinger, U. *Am. J. Physiol. Heart Circ. Physiol.* **2007**, *292*, H3198–3206.
(22) Lilledahl, M. B.; Haugen, O. A.; de Lange Davies, C.; Svaasand, L. O. *J. Biomed. Opt.* **2007**, *12*, 044005.
(23) Pena, A.-M.; Fabre, A.; Débarre, D.; Marchal-Somme, J.; Crestani, B.; Martin, J.-L.; Beaurepaire, E.; Schanne-Klein, M.-C. *Microsc. Res. Tech.* **2007**, *70*, 162–170.
(24) Strupler, M.; Hernest, M.; Fligny, C.; Martin, J.-L.; Tharaux, P.-L.; Schanne-Klein, M.-C. *J. Biomed. Opt.* **2008**, *13*, 054041.
(25) Strupler, M.; Pena, A.-M.; Hernest, M.; Tharaux, P.-L.; Martin, J.-L.; Beaurepaire, E.; Schanne-Klein, M.-C. *Opt. Express* **2007**, *15*, 4054–4065.
(26) Débarre, D.; Suppato, W.; Pena, A. M.; Fabre, A.; Tordjmann, T.; Combettes, L.; Schanne-Klein, M. C.; Beaurepaire, E. *Nat. Methods* **2006**, *3*, 47–53.
(27) Pena, A.-M.; Boulesteix, T.; Dartigalongue, T.; Schanne-Klein, M.-C. *J. Am. Chem. Soc.* **2005**, *127*, 10314–10322.
(28) Roth, S.; Freund, I. *Biopolymers* **1981**, *20*, 1271–1290.
(29) Stoller, P.; Celliers, P. M.; Reiser, K. M.; Rubenchik, A. M. *Appl. Opt.* **2003**, *42*, 5209–5219.
(30) Erikson, A.; ; Ortegren, J.; Hompland, T.; Davies, C. d. L.; Lindgren, M. *J. Biomed. Opt.* **2007**, *12*, 044002.
(31) Chu, S.-W.; Tai, S.-P.; Chan, M.-C.; Sun, C.-K.; Hsiao, I.-C.; Lin, C.-H.; Chen, Y.-C.; Lin, B.-L. *Opt. Express* **2007**, *15*, 12005–12010.
(32) Clays, K.; Persoons, A. *Phys. Rev. Lett.* **1991**, *66*, 2980–2983.
(33) Verbiest, T.; Clays, K.; Persoons, A.; Meyers, F.; Brédas, J. L. *Opt. Lett.* **1993**, *18*, 525.
(34) Zyss, J.; Van, T. C.; Dhenaut, C.; Ledoux, I. *Chem. Phys.* **1993**, *177*, 281.
(35) Gobeaux, F.; Belamie, E.; Mosser, G.; Davidson, P.; Panine, P.; Giraud-Guille, M.-M. *Langmuir* **2007**, *23*, 6411–6417.
(36) Bhatnagar, R. S.; Gough, C. A. *Circular Dichroism and the Conformational Analysis of Biomolecules*; Fasman, G. D., Ed.; Plenum Press: New-York, 1996; pp 183−199.
(37) Holmgren, S. K.; Taylor, K. M.; Bretscher, L. E.; Raines, R. T. *Nature* **1998**, *392*, 666–7.
(38) Li, S. T. *The Biomedical Engineering Handbook*; Bronzino, J. D., Ed.; CRC Press: 1995, pp 627−647.
(39) Roth, S.; Freund, I. *J. Chem. Phys.* **1979**, *70*, 1637–1643.
(40) Rocha-Mendoza, I.; Yankelevich, D. R.; Wang, M.; Reiser, K. M.; Frank, C. W.; Knoesen, A. *Biophys. J.* **2007**, *93*, 4433–44.
(41) Cyvin, S. J.; Rauch, J. E.; Decius, J. C. *J. Chem. Phys.* **1965**, *43*, 4083.
(42) Bersohn, R.; Pao, Y. H.; Frisch, H. L. *J. Chem. Phys.* **1966**, *45*, 3184.
(43) Nappa, J.; Revillod, G.; Russier-Antoine, I.; Benichou, E.; Jonin, C.; Brevet, P. F. *Phys. Rev. B* **2005**, *71*, 165407.
(44) Wu, Y.; Mao, G.; Li, H.; Petschek, R. G.; Singer, K. D. *J. Opt. Soc. Am. B* **2008**, *25*, 495.
(45) Brasselet, S.; Zyss, J. *J. Opt. Soc. Am. B* **1998**, *15*, 257–288.
(46) Van Der Rest, M.; Bruckner, P. *Curr. Opin. Struct. Biol.* **1993**, *3*, 430–436.
(47) Revillod, G.; Duboisset, J.; Russier-Antoine, I.; Benichou, E.; Bachelier, G.; Jonin, C.; Brevet, P.-F. *J. Phys. Chem. C* **2008**, *112*, 2716–2723.
(48) Fraser, R. D.; MacRae, T. P.; Suzuki, E. *J. Mol. Biol.* **1979**, *129*, 463–81.
(49) Vance, F. W.; Lemon, B. I.; Hupp, J. T. *J. Phys. Chem. B* **1998**, *102*, 10091.
(50) Williams, R. M.; Zipfel, W. R.; Webb, W. W. *Biophys. J.* **2005**, *88*, 1377–1386.
(51) Tiaho, F.; Recher, G.; Rouède, D. *Opt. Express* **2007**, *15*, 12286–12295.
(52) Han, X.; Burke, R. M.; Zettel, M. L.; Tang, P.; Brown, E. B. *Opt. Express* **2008**, *16*, 1846–1859.
(53) Ostroverkhov, V.; Petschek, R. G.; Singer, K. D.; Sukhomlinova, L.; Twieg, R. J.; Wang, S.-X.; Chien, L. C. *J. Opt. Soc. Am. B* **2000**, *17*, 1531–1542.
(54) Claire, K.; Pecora, R. *J. Phys. Chem. B* **1997**, *101*, 746–753.
(55) Okuyama, K.; Wu, G.; Jiravanichanun, N.; Hongo, C.; Noguchi, K. *Biopolymers* **2006**, *84*, 421–32.
(56) Maurice, D. M. *J. Physiol.* **1957**, *136*, 263–286.
(57) Plotnikov, S. V.; Millard, A. C.; Campagnola, P. J.; Mohler, W. A. *Biophys. J.* **2006**, 90.

Supporting information

A: Calculation of β_{eff} for $C_{\infty v}$ symmetry

Using expression (1) and setting $u' = \dfrac{\delta\beta_{zxx}}{\delta\beta_{zzz}}$, we obtain for the $C_{\infty v}$ symmetry:

$$\beta_{ZZZ} = \left[(\cos\theta)^3 + 3\cos\theta(\sin\theta)^2\ u'\right]\delta\beta_{zzz} \tag{A1}$$

$$\beta_{YZZ} = \left[(\cos\theta)^2\sin\theta\sin\varphi + \left((\sin\theta)^3\sin\varphi - 2(\cos\theta)^2\sin\theta\sin\varphi\right)u'\right]\delta\beta_{zzz} \tag{A2}$$

One then obtains equation (19): $\beta_{eff} = 3\,L\,K(L,u')\,\delta\beta_{zzz}$ with:

$$K^2(L,u') = \int_0^\pi d\theta\sin\theta\int_0^{2\pi} d\varphi\left[A + Bu' + Cu'^2\right]\operatorname{sinc}^2\left(\frac{k(2\omega)L}{2}(\sin\varphi - \cos\varphi)\sin\theta\right) \tag{A3}$$

In that equation, A, B and C reads:

$$A = \cos^6\theta + \cos^4\theta\sin^2\theta\sin^2\varphi \tag{A4}$$

$$B = 2\cos^2\theta\sin^2\theta\left(3\cos^2\theta\cos^2\varphi + \sin^2\varphi\right) \tag{A5}$$

$$C = 9\cos^2\theta\sin^4\theta + \sin^2\theta\sin^2\varphi\left(1 - 3\cos^2\theta\right)^2 \tag{A6}$$

B: Depolarization ratio of the collagen triple helix

Following Plotnikov et al [57] and other groups [51,52], we assume that elementary harmonophores are parallel to the peptidic scaffold and that they are characterized by a single $\delta\beta_{vvv}$ component along the direction v of the peptidic bond. The hyperpolarizabity tensor of a short triple helical domain is then calculated as the orientational averaging of the nonlinear response of those elementary harmonophores. For that purpose, we use the published structure of the collagen molecule: the peptidic scaffold exhibits an angle $\theta_1 = 45°$ from the α-chain axis and the 3 α-chains are aligned in the same direction and exhibit an angle $\theta_2 = 12°$ from the

triple helix axis.[7] The harmonophore's orientation is expressed in the triple helix frame by using twice the expression (1) to change from the peptidic frame to the α-chain frame and then from the α-chain frame to the triple helix frame. Azimuthal angles are considered as evenly distributed among the N harmonophores in the short triple helical domain because of the helical geometry. We then obtain as expected a $C_{\infty v}$ symmetry with the following tensor components:

$$\delta\beta_{zzz} = N\left[\cos^3\theta_1 \; \cos^3\theta_2 + 3/2 \cos\theta_1 \; \cos\theta_2 \sin^2\theta_1 \sin^2\theta_2\right]\delta\beta_{vvv} \tag{A7}$$

$$\delta\beta_{zxx} = N\left[\frac{\cos\theta_1 \; \cos\theta_2}{4}\left(2\sin^2\theta_1 + 2\sin^2\theta_2 - 5\sin^2\theta_1 \sin^2\theta_2\right)\right]\delta\beta_{vvv} \tag{A8}$$

Calculation of the ratio using $\theta_1 = 45°$ and $\theta_2 = 12°$ yields $u = 0.48$.